

Characterization of X-ray charge neutralizer using carbon-nanotube field emitter

Shuhei Okawaki, Satoshi Abo, Fujio Wakaya,^{a)} Hayato Yamashita, Masayuki Abe, and Mikio Takai

Graduate School of Engineering Science, Osaka University, Toyonaka, Osaka 560-8531 Japan

(Dated: Dec. 9, 2015 submitted to Jpn. J. Appl. Phys; revised on March 31, 2016)

An X-ray charge neutralizer using a screen-printed carbon-nanotube field emitter is demonstrated to show the possibility of a large-area flat-panel charge neutralizer, although the device dimensions in the present work are not very large. The X-ray yields and spectra are characterized to estimate the ion generation rate as one of the figures of merit of neutralizers. Charge neutralization characteristics are measured and show good performance.

Journal reference: Jpn. J. Appl. Phys. **55**, 06GF10 (2016) DOI: 10.7567/JJAP.55.06GF10

I. INTRODUCTION

It is widely known that static electricity causes troubles not only in high-tech industries but also in many fields including the manufacture of plastic, rubber, powder, and paper, and industries of textile, spinning, and printing, meaning that the management of static electricity has been important in many industries for a long time.^{1,2} In the ULSI industry, the device dimensions become continuously small³, leading to a more fragile device against static electricity. In the industry of flat-panel displays, the screen size and pixel dimension become continuously large and small, respectively, meaning that the product becomes more sensitive to particle contaminations caused by static electricity. These outstanding trends in high-tech industries suggest that the management of static electricity becomes more critical presently.

Although material modification by antistatic additive doping or surface coating is effective for overcoming static electricity problems¹, such a technique cannot always be adopted because, especially for electronic devices, an insulating material is necessary in many cases for realizing device functions. Charge neutralizers using air molecules ionized by corona discharge or soft X-ray irradiation are, therefore, often used for solving static electricity problems.^{1,2,4–8}

Corona-discharge-type charge neutralizers have the following disadvantages, although they are widely used:² (1) the charge balance of ionized air is not good, (2) the discharge process generates particles and causes contamination problems, (3) the density of ionized air is low on the target material surface, although it is high around the discharge electrodes, (4) the discharge process generates electromagnetic noise that may cause troubles in the target devices to be neutralized. The X-ray charge neutralizer has advantages concerning all the above problems. Particularly when the X-ray source is shaped to a large-area flat panel, it should be useful for present large-area flat-panel devices because of the uniform ion density over a large area.

A carbon nanotube (CNT) is one of the promising materials for electron field emitters owing to its high aspect ratio, high

current tolerance, high mechanical strength, and high chemical stability.^{9–11} Many applications using CNTs as field emitters, such as a field emission display,^{12,13} a backlight unit for a liquid crystal display,^{14,15} and an X-ray source,^{16–18} are reported. A screen-printed CNT mat with appropriate post surface treatments is one of the best candidates for realizing a large-area field emitter^{19–29} and can be applied to a large-area X-ray source^{18,30}. Although the X-ray generated at the large-area source may not be very suitable for high-resolution X-ray imaging, it should be useful for realizing a large-area X-ray charge neutralizer for large-area flat-panel devices.

In this study, an X-ray charge neutralizer using a screen-printed CNT cathode is demonstrated. Characterization results show good performance for a charge neutralizer.

II. EXPERIMENTAL METHODS

To apply electron field emitters to an X-ray source, a three-terminal configuration with emitters, gate electrodes, and an anode is necessary; such a configuration enables us to control separately the anode current from the anode voltage, leading to the separate control of the X-ray intensity and X-ray energy. An in-plane side-gate structure is adopted in the present work because it is easily applied to a large-area flat-panel emitter. The fabrication process for the emitter, which was already reported,^{28–30} is summarized as below. Indium-tin-oxide (ITO) electrodes of $30 \times 1 \text{ mm}^2$, some of which were used as side-gate electrodes and others as back electrodes for CNT cathodes, were deposited on a glass substrate. A CNT paste was screen-printed on a part of the ITO electrodes with an area of $10 \times 1 \text{ mm}^2$. The gap between the edges of the CNT cathode and side-gate electrode is $100 \mu\text{m}$. The schematic top view of the cathode is shown in Fig. 1. The effective area of the cathode, which is $\sim 4 \times 10 \text{ mm}^2$, is not very large but it can easily be enlarged because screen printing can easily be applied to a large-area process. The tape-peeling surface treatment was performed to improve the electron emission property.^{26,27}

The experimental setup used to generate and detect X-rays is schematically shown in Fig. 2. In a vacuum of $\sim 10^{-5} \text{ Pa}$, a $10\text{-}\mu\text{m}$ -thick Cu thin film, placed 8 cm away from the emitter, was irradiated by field-emitted electrons from the CNT cathode typically at 10 keV to generate X-rays. To characterize

^{a)}Corresponding author: wakaya@stec.es.osaka-u.ac.jp

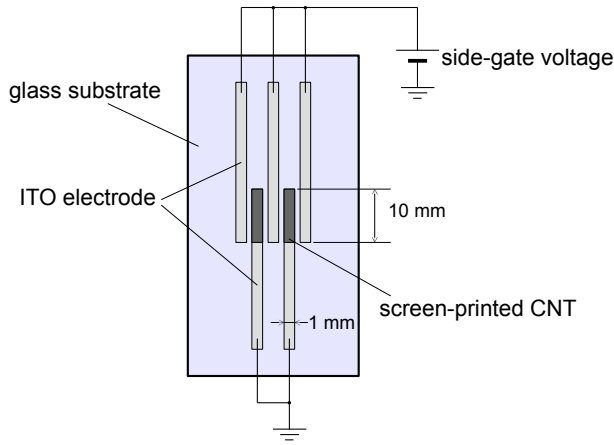


FIG. 1. (Color online) Schematic top view of screen-printed CNT cathode with side-gate electrodes. The bias setup for extracting electrons is also shown.

the X-ray spectrum and yield in vacuum, the X-ray detector was set 4 cm away from the Cu film as shown in Fig. 2(a). To characterize X-rays in air, a 250- μm -thick Be window was used and the X-ray detector was set in air 5 cm away from the Be window shown in Fig. 2(b). The X-ray detection system used is Amptek XR-100CR/PX4 with a detector area of 13 mm².

Ion current was measured in air by a metal plate of 40 \times 40 mm², placed 5 cm away from the Be window instead of the X-ray detector shown in Fig. 2(b). The bias voltage of the plate was kept constant at -1 kV during the measurement. This is not exactly the same as the real neutralization situation, because the voltage of the object material decreases during the real neutralization process. Such a technique, however, is often used for characterizing charge neutralizers.² Charge neutralization performance as a function of time was characterized by using the charged plate monitor shown schematically in Fig. 3 placed in air 5 cm away from the Be window. The area and capacitance of the charged plate monitor are 25 \times 25 mm² and 25 pF, respectively. The current I_{gr} defined in Fig. 3 was measured as a function of time t , since the high-voltage source was disconnected from the circuit. The electric potential of the charged plate, V_{cp} , can be estimated as

$$V_{\text{cp}}(t) = V_{\text{cp}}(0) - \frac{1}{C} \int_0^t I_{\text{gr}} dt, \quad (1)$$

with $V_{\text{cp}}(0) = 5$ kV and $C = 25$ pF. The direct measurement of V_{cp} is difficult because the ion current and I_{gr} are typically 10^{-9} A at the electric potential of 10^3 V as discussed in the following section, which means that a voltmeter input impedance of more than 10^{12} Ω is necessary. This is the reason why the estimation using Eq. (1) is adopted in this work.

III. RESULTS AND DISCUSSION

The anode current of the CNT cathode with side-gate electrodes was controlled by the side-gate voltage and reached the

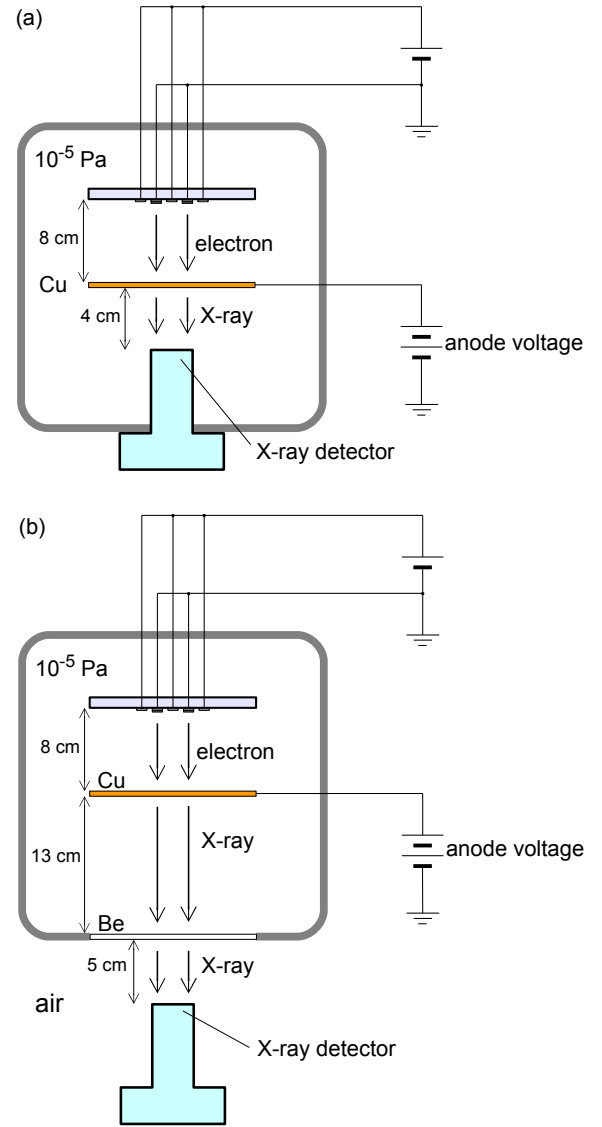


FIG. 2. (Color online) Experimental setup for generating and detecting X-rays. The X-ray detector is placed in vacuum (a) or in air (b).

highest value of 300 μA . The detailed field-emission properties were similar to those observed in the previous work³⁰.

Figure 4 shows the X-ray spectra obtained in vacuum, the setup for which is shown in Fig. 2(a). The anode current during the measurement was reduced and kept at 1 nA, although it can be increased up to 300 μA as described previously, because the X-ray spectrum cannot be measured if it is very strong. The characteristic X-ray peaks of Cu were observed when the anode voltage was 10 kV. For all anode voltages, the maximum energy of the bremsstrahlung X-ray corresponded to the anode voltage as expected.

The X-ray spectra obtained in air are shown in Fig. 5. When the spectrum was measured in air, the X-ray was absorbed by air and its intensity decreased. The anode current was, therefore, increased to 400 nA, while the other parameters were maintained the same as in the in-vacuum measurement shown in Fig. 4. The maximum energies of the bremsstrahlung X-

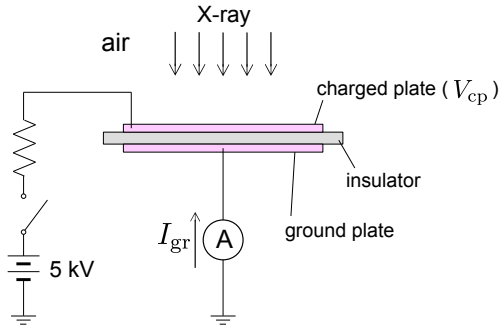


FIG. 3. (Color online) Schematic of charged plate monitor with measurement setup.

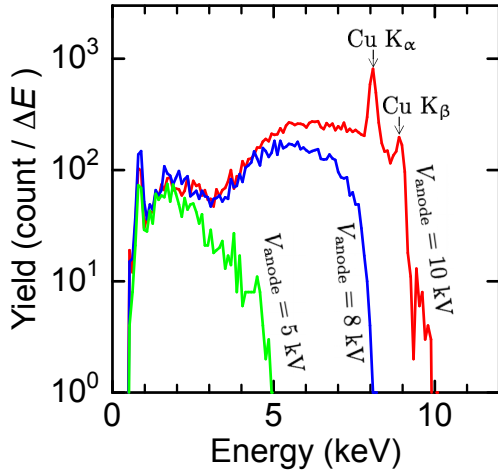


FIG. 4. (Color online) Energy spectra of X-rays measured in vacuum as in Fig. 2(a). The channel width ΔE of the multichannel analyzer is 89.9 eV. The anode current is fixed to 1 nA during the measurement. The measurement time for each spectrum is 60 s.

rays with anode voltages of 8 and 10 kV exceed the corresponding anode voltages not as expected. This is due to the double or multiple counting of photons during the time constant of the detection system.

For the charge neutralizer, the ion generation rate G is one of the important figures of merit, which can be estimated as

$$G(T, P) = \frac{1}{S \Delta t} \sum_i \frac{E_i}{W} Y(E_i) \left[\frac{\mu_{\text{en}}(E_i)}{\rho} \right] \rho(T, P), \quad (2)$$

where T and P are the air temperature and pressure, respectively, S is the area of the X-ray detector, Δt is the measurement time for obtaining the spectrum, E_i is the X-ray energy of the i th channel of the detector, W is the average ionization energy of air, $Y(E_i)$ is the X-ray yield, $\mu_{\text{en}}(E_i)$ is the X-ray absorption coefficient of air, ρ is the mass density of air. Figure 6 shows the ion generation rate estimated from the spectrum shown in Fig. 5 using Eq. (2) with $S = 13 \text{ mm}^2$, $\Delta t = 60 \text{ s}$, $W = 34 \text{ eV}$,^{31,32} μ_{en}/ρ from the database,³³ and $\rho = 1.205 \times 10^{-3} \text{ g/cm}^3$ at 760 Torr and 20 °C.³⁴ The maximum ion generation rate in Fig. 6 is $1.6 \times 10^5 \text{ cm}^{-3}\text{s}^{-1}$, corresponding

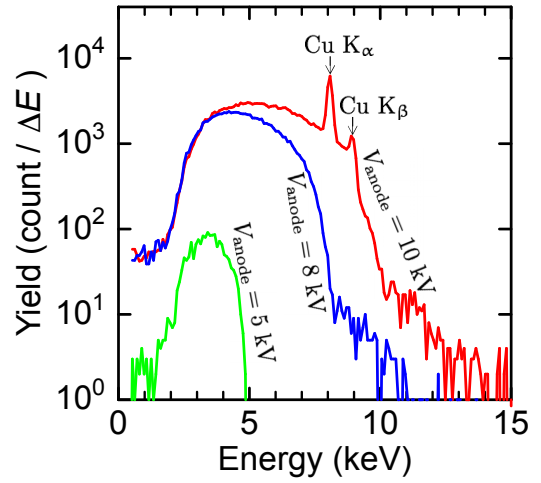


FIG. 5. (Color online) Energy spectra of X-ray measured in air as in Fig. 2(b). The channel width ΔE of the multichannel analyzer is 89.9 eV. The anode current is fixed to 400 nA during the measurement. The measurement time for each spectrum is 60 s.

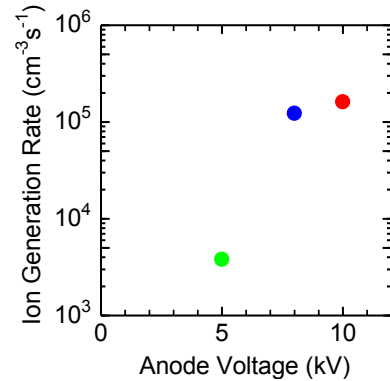


FIG. 6. (Color online) Estimated ion generation rate at 760 Torr and 20 °C as a function of anode voltage.

to the ion concentration C_{ion} of $5.0 \times 10^5 \text{ cm}^{-3}$.⁷ It is reported⁷ that $C_{\text{ion}} = 10^7 \text{ cm}^{-3}$ or $G = 6.3 \times 10^7 \text{ cm}^{-3}\text{s}^{-1}$ is enough for a charge neutralizer. The maximum G estimated in the present work is two orders of magnitude lower than this value. The ion generation rate can, however, be increased by increasing the anode current, which was intendedly reduced from 300 μA to 400 nA in order to obtain the X-ray spectrum shown in Fig. 5. Assuming that G is proportional to the anode current, we can expect G to be 750 times larger than those in the present work with an anode current of 300 μA , the upper limit of the emitter used in the present work. This means that the charge neutralization performance of the present device is fairly good.

The ion currents observed in air by using the metal plate biased at -1 kV are shown in Fig. 7 as a function of the anode current. The ion current was roughly proportional to the anode current as expected. The absolute value of ion current with positive bias should be similar because it is considered that the ion balance of the X-ray charge neutralizer is better

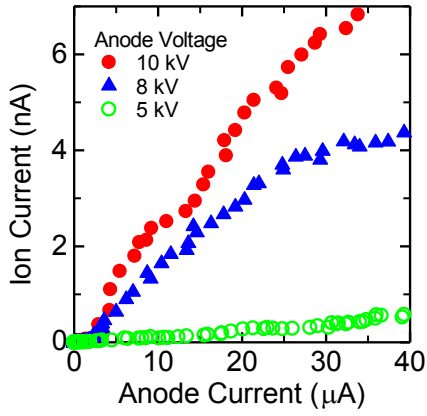


FIG. 7. (Color online) Ion current measured in the air as a function of anode current.

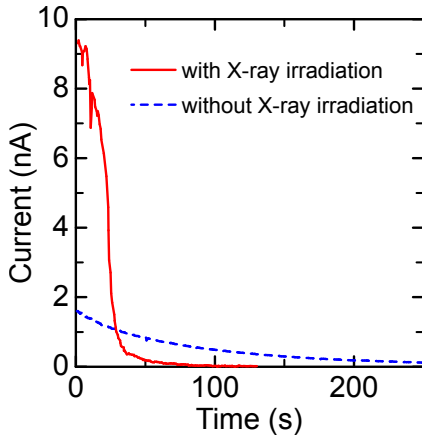


FIG. 8. (Color online) Current measured by the charged plate monitor shown in Fig. 3. The distance between the Be window and the charged plate is 5 cm. The anode voltage and anode current were 10 kV and 300 μ A, respectively, during the measurement.

than that of the corona-discharge-type neutralizer², although the measurement with positive bias was not performed owing to the voltage source restriction.

The measured current to the ground plate I_{gr} , defined in Fig. 3, is shown in Fig. 8. For this measurement, the anode current was increased and fixed to 300 μ A to obtain the highest neutralization performance. When the current I_{gr} shown in this figure is used with Eq. (1), $V_{cp} \neq 0$ after a sufficiently long time. This is probably due to the unreliable value of the capacitance C . If C is assumed to be $\sim 10\%$ larger than 25 pF, $V_{cp} = 0$ after a sufficiently long time. The following normalization was, therefore, used instead of Eq. (1) to avoid the problem:

$$V_{cp}(t) = V_{cp}(0) \left(1 - \frac{\int_0^t I_{gr} dt}{\int_0^\infty I_{gr} dt} \right). \quad (3)$$

The resulting estimated electronic potentials at the charged plate with and without X-ray irradiation are shown in Fig. 9.

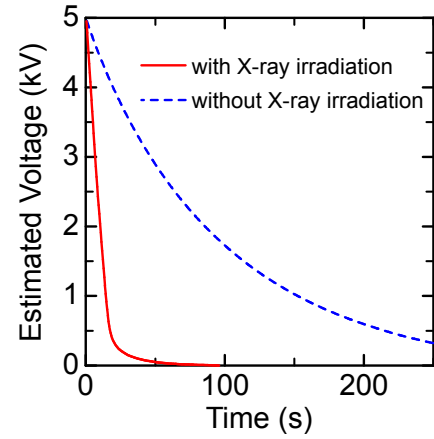


FIG. 9. (Color online) Voltage at the charged plate as a function of time estimated from the observed current shown in Fig. 8.

The decay observed without X-ray irradiation should be due to the natural neutralization of the charged plate interacting with the surrounding air. If the decay time is defined as the time at which the voltage becomes 1/10 of the initial value, it is estimated to be 17.5 and 215 s with and without X-ray irradiation, respectively. The decay time of 17.5 s with X-ray irradiation is not very good compared with the reference⁷, but can be improved by increasing the X-ray intensity. The X-ray intensity can be increased by decreasing the distances between the Cu target and the Be window and between the Be window and the object material to be neutralized, which are 13 and 5 cm, respectively, in the present work for the preliminary demonstration.

IV. CONCLUSIONS

An X-ray charge neutralizer was demonstrated by using a screen-printed CNT field emitter. The effective area of the emitter is $\sim 4 \times 10 \text{ mm}^2$. This is not very large and is almost a point source because the distances in the present work between the emitter and the Cu target, between the Cu target and the Be window, and between the Be window and the object material to be neutralized are 8, 13, and 5 cm, respectively. To realize a large-area flat-panel source is not difficult because screen printing can be easily applied to a large-area process. Charge neutralization characteristics were measured and showed good performance even under such an almost point-source condition, suggesting that the performance is much improved when a vacuum-sealed large-area flat-panel charge neutralizer is realized using the screen-printed CNT field emitter.

ACKNOWLEDGMENTS

This work was partially supported by JSPS KAKENHI Grant Number 23360022.

- ¹C. G. Noll, in *Handbook of Electrostatic Processes*, ed. J.-S. Chang, A. J. Kelly, and J. M. Crowley, (Marcel Dekker, New York, 1995) Chap. 33.
- ²*Seidenki Joden no Sochi to Gijutsu* (Ionizer and Tehnique of Charge Eliminating), ed. Y. Murata (CMC, Tokyo, 2004) [in Japanese].
- ³International Technology Roadmap for Semiconductors 2013 Edition Executive Summary (2013) [<http://www.itrs.net>].
- ⁴K.-S. Choi, T. Fujiki, and Y. Murata, *Jpn. J. Appl. Phys.* **43**, 7693 (2004).
- ⁵K.-S. Choi, S. Nakamura, and Y. Murata, *Jpn. J. Appl. Phys.* **44**, 3248 (2005).
- ⁶H. Inaba, T. Ohmi, T. Yoshida, and T. Okada, *J. Electrostat.* **33**, 15 (1994).
- ⁷H. Inaba, T. Ohmi, T. Yoshida, and T. Okada, *IEICE Trans. Electron.* **E79-C**, 328 (1996).
- ⁸J. Kawai, H. Ishii, and Y. Hosokawa, *Int. Symp. Discharges and Electrical Insulation in Vacuum*, 2006, Vol. 2, p. 628.
- ⁹S. Iijima, *Nature* **354**, 56 (1991).
- ¹⁰W. A. de Heer, A. Châtelain, and D. Ugarte, *Science* **270**, 1179 (1995).
- ¹¹P. G. Collins and A. Zettl, *Appl. Phys. Lett.* **69**, 1969 (1996).
- ¹²Q. H. Wang, M. Yan, and R. P. H. Chang, *Appl. Phys. Lett.* **78**, 1294 (2001).
- ¹³W. B. Choi, Y. W. Jin, H. Y. Kim, S. J. Lee, M. J. Yun, J. H. Kang, Y. S. Choi, N. S. Park, N. S. Lee, and J. M. Kim, *Appl. Phys. Lett.* **78**, 1547 (2001).
- ¹⁴Y. C. Kim and E. H. Yoo, *Jpn. J. Appl. Phys.* **44**, L454 (2005).
- ¹⁵Y. C. Kim, H. S. Kang, E. Cho, D. Y. Kim, D. S. Chung, I. H. Kim, I. T. Han, and J. M. Kim, *Nanotechnology* **20**, 095204 (2009).
- ¹⁶H. Sugie, M. Tanemura, V. Filip, K. Iwata, K. Takahashi, and F. Okuyama, *Appl. Phys. Lett.* **78**, 2578 (2001).
- ¹⁷J.-W. Jeong, J.-W. Kim, J.-T. Kang, S. Choi, S. Ahn, and Y.-H. Song, *Nanotechnology* **24**, 085201 (2013).
- ¹⁸T. Manabe, S. Nitta, S. Abo, F. Wakaya, and M. Takai, *J. Vac. Sci. Technol. B* **31**, 02B110 (2013).
- ¹⁹W.-J. Zhao, A. Sawada, and M. Takai, *Jpn. J. Appl. Phys.* **41**, 4314 (2002).
- ²⁰W. J. Zhao, N. Kawakami, A. Sawada, and M. Takai, *J. Vac. Sci. Technol. B* **21**, 1734 (2003).
- ²¹W. J. Zhao, W. Rochanachivapar, and M. Takai, *J. Vac. Sci. Technol. B* **22**, 1315 (2004).
- ²²A. Sawada, M. Iriguchi, W. J. Zhao, C. Ochiai, and M. Takai, *J. Vac. Sci. Technol. B* **21**, 362 (2003).
- ²³Y. Kanazawa, T. Oyama, K. Murakami, and M. Takai, *J. Vac. Sci. Technol. B* **22**, 1342 (2004).
- ²⁴W. Rochanachirapar, K. Murakami, N. Yamasaki, S. Abo, F. Wakaya, M. Takai, A. Hosono, and S. Okuda, *J. Vac. Sci. Technol. B* **23**, 765 (2005).
- ²⁵K. Ohsumi, T. Honda, W. S. Kim, C. B. Oh, K. Murakami, S. Abo, F. Wakaya, M. Takai, S. Nakata, A. Hosono, and S. Okuda, *J. Vac. Sci. Technol. B* **25**, 557 (2007).
- ²⁶H. Oki, A. Kinoshita, T. Takikawa, W. S. Kim, K. Murakami, S. Abo, F. Wakaya, and M. Takai, *J. Vac. Sci. Technol. B* **27**, 761 (2009).
- ²⁷T. Takikawa, H. Oki, Y. Matsuura, K. Murakami, S. Abo, F. Wakaya, and M. Takai, *J. Vac. Sci. Technol. B* **28**, C2C41 (2010).
- ²⁸T. Manabe, S. Nitta, S. Abo, F. Wakaya, and M. Takai, *Tech. Dig. 25th Int. Vacuum Nanoelectronics Conf. (IVNC 2012)*, p. 122.
- ²⁹S. Nitta, S. Abo, F. Wakaya, and M. Takai, *Proc. Int. Display Workshop 2012*, Vol. 19, p. 1765.
- ³⁰S. Okawaki, S. Abo, F. Wakaya, M. Abe, and M. Takai, *Jpn. J. Appl. Phys.* **54**, 06FF10 (2015).
- ³¹*Houshasen Gairon* (Introduction to Radiation), ed. H. Iida (Tsusho Sangyo Kenkyusha, Tokyo, 2005) 6 ed. [in Japanese].
- ³²S. Macheret, M. Shneider, and R. Miles, *IEEE Trans. Plasma Sci.* **30**, 1301 (2002).
- ³³J. H. Hubbell and S. M. Seltzer, "Tables of X-Ray Mass Attenuation Coefficients and Mass Energy-Absorption Coefficients from 1 keV to 20 MeV for Elements Z = 1 to 92 and 48 Additional Substances of Dosimetric Interest" (2004) [<http://www.nist.gov/pml/data/xraycoef/index.cfm>].
- ³⁴*Rika Nenpyo* (Chronological Scientific Tables), ed. National Astronomical Observatory of Japan, (Maruzen, Tokyo, 1990) [in Japanese].